THE ROLE OF VORTICITY IN TURBULENT, RECTANGULAR, FREE AND WALL JETS

Thrassos Panidis

Mechanical Engineering and Aeronautics Department, University of Patras, 26504 Rio-Patras, Greece
panidis@upatras.gr

Andrew Pollard

Department of Mechanical and Materials Engineering, Queen's University Kingston, K7L-3N6 Ontario, Canada
andrew.pollard@queensu.ca

Rainer Schwab

Department of Mechanical and Materials Engineering, Queen's University Kingston, K7L-3N6 Ontario, Canada

ABSTRACT

Experimental results on the near field development of a rectangular jet with aspect ratio 10 are presented. The jet issues from a sharp-edged orifice attached to a rectangular settling chamber at $Re_{Dh} \sim 42{,}000$ either in free space or parallel to a flat wall. Measurements on cross plane grids obtained with a two-component hot wire anemometry probe, provide information on the three-dimensional characteristics of the flow field. Data were suitably averaged over the symmetrical areas of each cross section. Mean vorticity components and terms of the axial vorticity equation were estimated by interpolation and derivation of the mean velocity measurements. Key features of this type of jet are saddleback mean axial velocity profiles and a predominant dumbbell shape of the axial mean velocity contours. These characteristics are found to be influenced by the axial vorticity distribution, which is related to two terms in the axial mean vorticity transport equation that diffuse fluid from the center of the jet towards its periphery.

INTRODUCTION

Rectangular free and wall jets have attracted the interest of researchers for many years, since they belong to a class of shear flows which is important for understanding the fundamentals of turbulence but also constitute a generic flow configuration in engineering applications. In the past, experimental studies focussed on the global characteristics of jet velocity decay, growth, the entrainment process and the shape of the mean and turbulent profiles up to the self-similarity zone, while more recent studies focus on the influence of specific inlet and boundary conditions, including aspect ratio, nozzle exit geometry and external boundaries along with the Reynolds number on jet development (see Vouros et al. 2015 and Agelin-Chaab, 2010 for recent reviews). Rectangular free and wall jets present important three dimensional characteristics and although quite early Launder and Rodi (1983) noticed the importance of variables such as the axial vorticity, the available experimental information is rather scarce. Nowadays, it is clear that in order to capture the 3D characteristics of rectangular jets, measurements of the velocity and the vorticity in a volume, i.e. on suitable cross plane grids are required.

In this work measurements of the three velocity components, obtained with X-probe hot wire anemometry, on cross plane grids in a free and a wall jet (Schwab, 1986), are further exploited using modern interpolation techniques. The jets are issuing under identical conditions from a 1:10 aspect ratio, sharp-edged, rectangular orifice, at $Re_h \sim 23{,}000$ based on slot height, h ($Re_{Dh} \sim 42{,}000$, based on the hydraulic diameter, D_h), indicating that the jets should be fully turbulent, at least beyond the near field (Dimotakis, 2000, Fellouah and Pollard, 2009). The expected symmetries of the distributions are imposed on the experimental data by suitable averaging, taking into account the symmetry properties of each variable. Mean vorticity components and terms of the axial vorticity budget equation are estimated by interpolation and derivation from the mean velocity measurements (Vouros et al. 2015, Panidis et al. 2016). Contour plots of flow characteristics including mean velocity components, normal and shear Reynolds stresses, mean vorticity components and terms of the vorticity budget are presented in the following to discuss the complex underlying flow physics. The configuration of the orifice and the Cartesian coordinate grid used in this work are depicted in fig. 1. In all the following contour plots, a rectangular indicates the location of the exit orifice whereas, black contour lines correspond to streamwise velocity values U/U_{cl}= 0.5, 0.95 and in some cases 1.05, where U_{cl} is the local centreline velocity.

VELOCITY FIELD

The axial velocity distributions of the free jet (Fig. 2.a) present several of the features characterizing sharp-edged

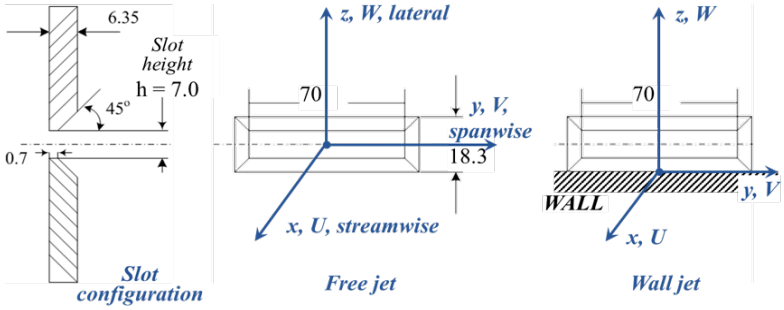

Figure 1. Free and wall jet configurations and coordinate systems

rectangular jets of high aspect ratio. The $U/U_{cl} = 0.5$ contour indicates that the jet initially contracts in both directions (close to jet exit, vena contracta effect) whereas downstream an axis switching effect is observed, since the jet is contracting in the spanwise direction and spreading in the lateral one. This phenomenon is associated with the dumbbell shape of the jet outline (also observed in visualisations) and the development of saddle back profiles, with peak velocity values observed at locations close to the spanwise edges of the jet, symmetrically to the jet central axis. In the case of the wall jet (Fig. 2.a) the development of the dumbbell shape and the saddle back profile is constrained by the presence of the wall. The smoothing out of the two velocity peaks is delayed, whereas a Coanda effect attracts the jet towards the wall, as indicated by the displacement of velocity peaks towards the wall downstream. Complementing information on the development of the flow field is provided by the cross plane velocity components. The spanwise mean velocity plots (Fig. 2.b) in the case of the free jet clearly depict the contraction of the jet in the spanwise direction. In the case of the wall jet the velocity field leading to the contraction in the spanwise direction is also evident. Moreover, in these figures an outward velocity field is seen to develop in the outer limits of the jet at the farthest from the exit locations. Correspondingly, the lateral velocity component (Fig. 3.a) in the case of the free jet, is compatible with the jet lateral spreading in both direction, whereas, in the case of the wall jet higher velocities indicative of jet spreading in the direction away from the wall are observed.

The axial turbulent intensity peak values (Fig. 3.b, and consequently those of the corresponding normal Reynolds stress), are associated with the shear layers developing between the jet and the ambient or the wall in the case of the wall jet while, in the early stages, a "potential core" with very low values can be identified. The patterns are similar for the other two turbulent intensity components (not presented here). In general, values are higher for the axial component followed by those in the lateral, z, direction. In the case of the wall jet the values in the shear layer between the jet and the ambient are higher than in the free wall case, whereas those in the wall shear layer become weak downstream.

The uv shear stress (Fig. 4.a) in the initial stages takes peak values in the shear layers close to the spanwise edges of the jet, changing sign across lines in the lateral direction, associated with the off-center peaks of the axial velocity. At the farthest location, there is only one change of sign across a line in the lateral direction passing through the center of the jet. The presence of the wall affects the pattern of the distributions. The change of sign is

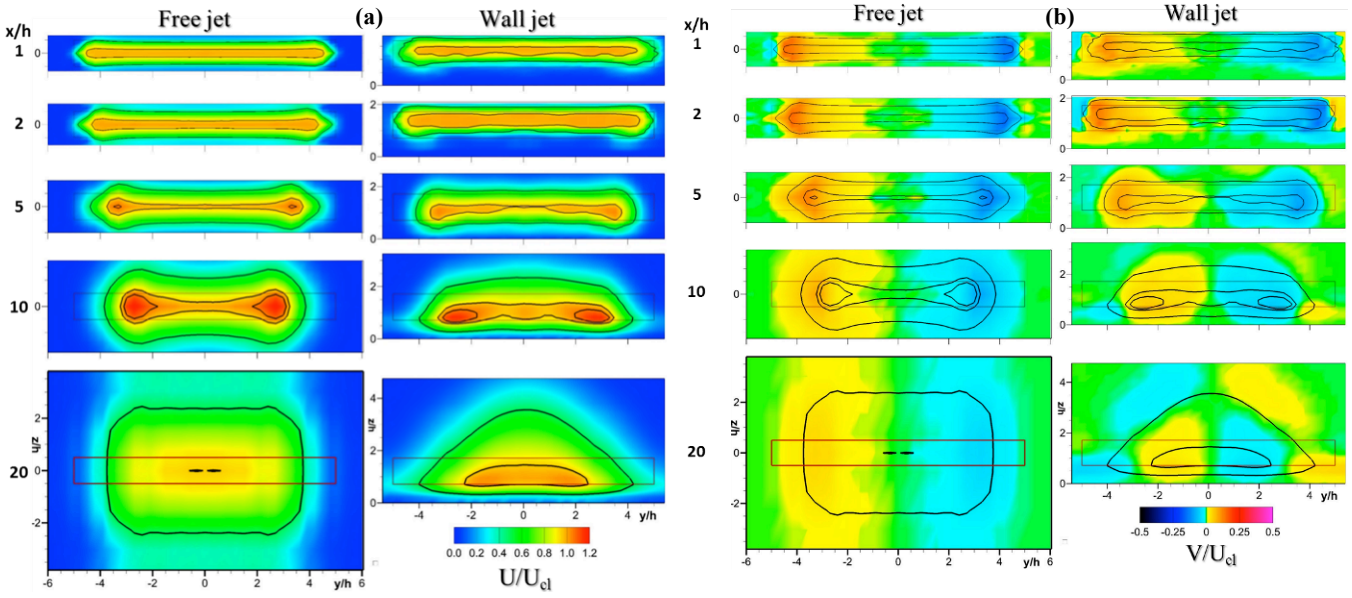

Figure 2. Contour plots on cross planes at distances x/h from exit: (a) Axial mean velocity, U/U_{cl}, (b) Spanwise mean velocity, V/U_{cl} .

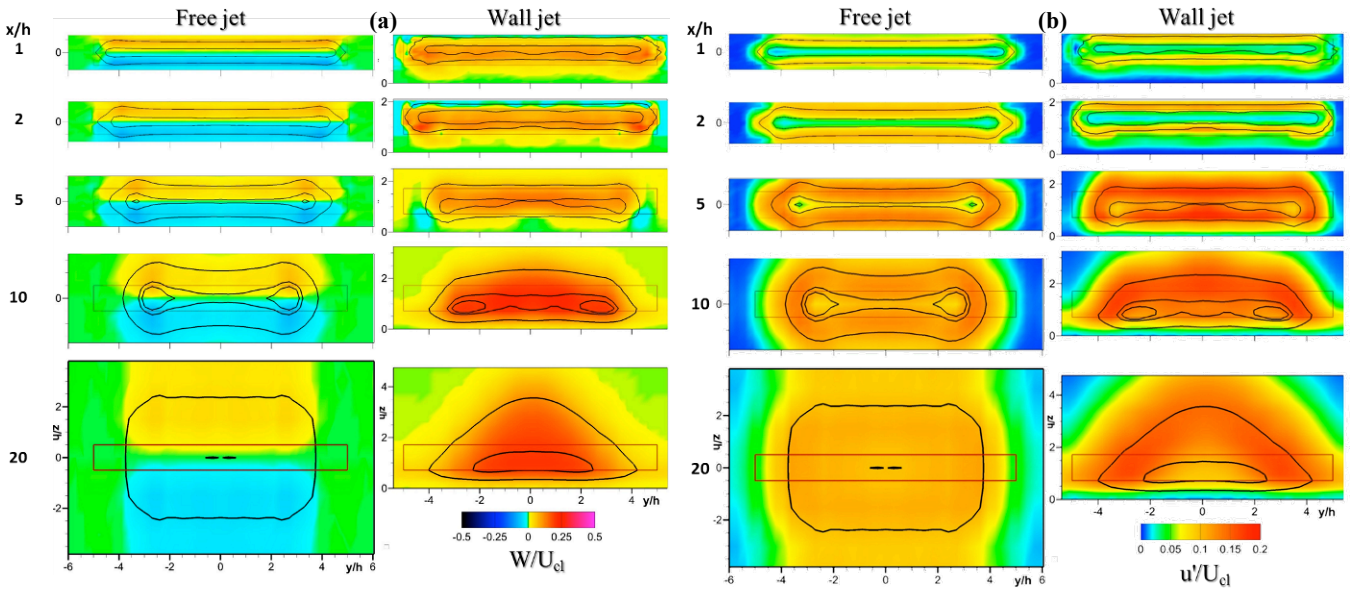

Figure 3. Contour plots on cross planes at distances x/h from exit: (a) Lateral mean velocity, W/U_{cl}, (b) Axial turbulence intensity u'/U_{cl}.

quickly shifted to the center of the jet in the area along the spanwise axis whereas, the sign is also changing across the lateral edges. This process results in the final stage in a pattern similar to that of the free jet, with the exception of a small area close to the wall, where values of inverse sign are observed.

Corresponding patterns are seen in the uw stress distributions (Fig. 4.b). In the initial stages, peak values of opposite signs are observed in the shear layers close to the lateral edges of the jet, while almost zero values prevail in the "potential core". Downstream, as the potential core is consumed, the area of zero values decreases and the change of sign takes place across the spanwise (large) axis of the jet. In the case of the wall jet, the contour plots are similar to those of the free jet in the initial stages. Downstream, the positive uw values in the outer shear layer attain significantly higher values whereas, negative values in the close to the wall, inner shear layer, are gradually restricted to smaller areas and finally disappear.

VORTICITY FIELD

The total mean vorticity magnitude (Fig. 5.a), seems to be dominated by the streamwise velocity shear layers developing along the periphery of the jet for both the free and the wall jet. In the early stages of development peak values are almost aligned with the $U/U_{cl} = 0.5$ contour. Farther from the jet exit, in the case of the free jet, the short side shear layers are associated with higher total vorticity magnitude values whereas, in the case of the wall jet high values are also observed within the shear layer

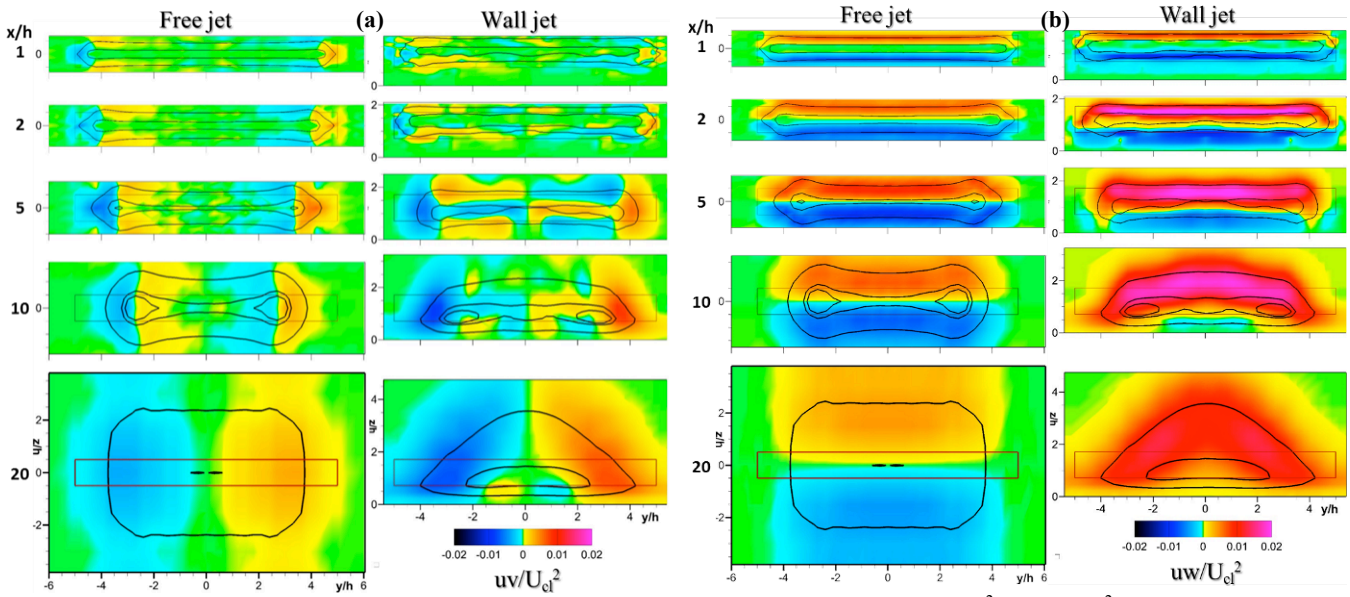

Figure 4. Contour plots of Reynolds shear stresses on cross planes at distances x/h from exit: (a) uv/U_{cl}^2, (b) uw/U_{cl}^2.

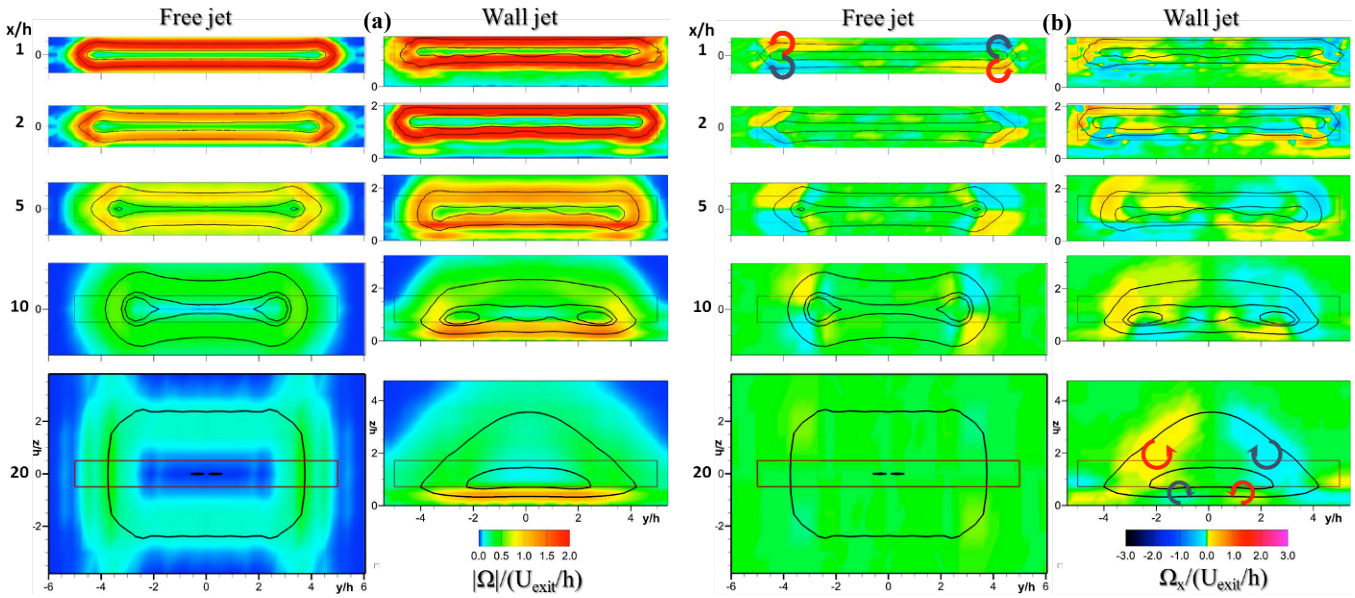

Figure 5. Contour plots on cross planes at distances x/h from exit: (a) Vorticity magnitude $|\Omega|/(U_{exit}/h)$, (b) Streamwise vorticity, $\Omega_x/(U_{exit}/h)$.

developing close to the wall, which gradually become dominant.

Specific to high aspect ratio jets, emanating from a sharp edged rectangular orifice, attached to a square cross section settling chamber is believed to be the development of a system of four vortices with alternating positive and negative axial vorticity (Ω_x, Fig. 5.b), developing at the four corners of the orifice at exit plane, probably due to the unequal contraction from the settling chamber to the jet orifice. In the case of the free jet, these vortices seem to affect the development of the dumbbell shape and the saddleback profiles and at intermediate distances from jet exit, weaker vortices of alternating vorticity sign develop on the other sides of the velocity peaks, whereas farther downstream the vortices are hardly discernible. In the case of the wall jet, the wall imposes an additional vorticity source and a distorted system of vortices prevails downstream. The two vortices on the wall side of the jet are progressively displaced towards the wall centre and at the last station two counter rotating vortices close to the centre of the wall and two vortices with opposite vorticity, associated with the outer shear layer, are observed.

The transverse vorticity components (Fig. 6.a, b) are mainly affected by the shear layers associated with the axial mean velocity distributions. In the free jet case, the Ω_y component attains high positive or negative values along the long side shear layers, due to the streamwise velocity gradients in z direction, whereas the Ω_z component is affected by the gradients in y direction, along the short sides' shear layers of the jet. The distributions for the wall jet present similar features in the first stations. The development of a wall shear layer results in the appearance of high values of Ω_y close to the wall. The displacement of the wall side axial vorticity vortices, discussed

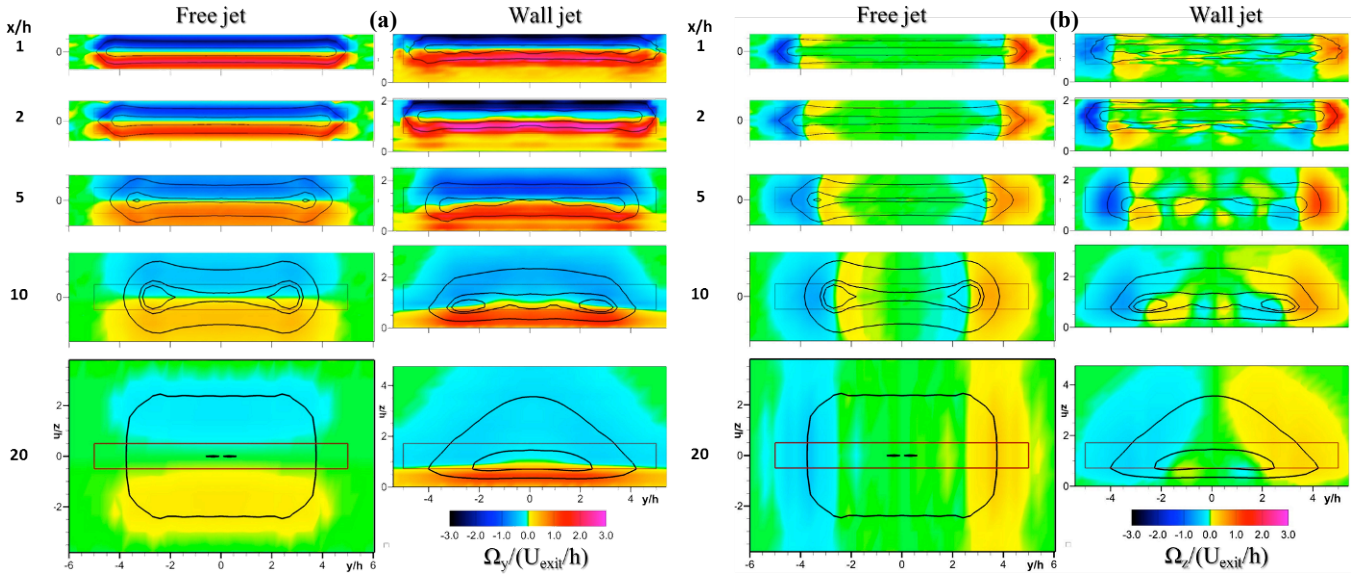

Figure 6. Contour plots on cross planes at distances x/h from exit: (a) Spanwise vorticity $\Omega_y/(U_{exit}/h)$, (b) Lateral vorticity, $\Omega_z/(U_{exit}/h)$

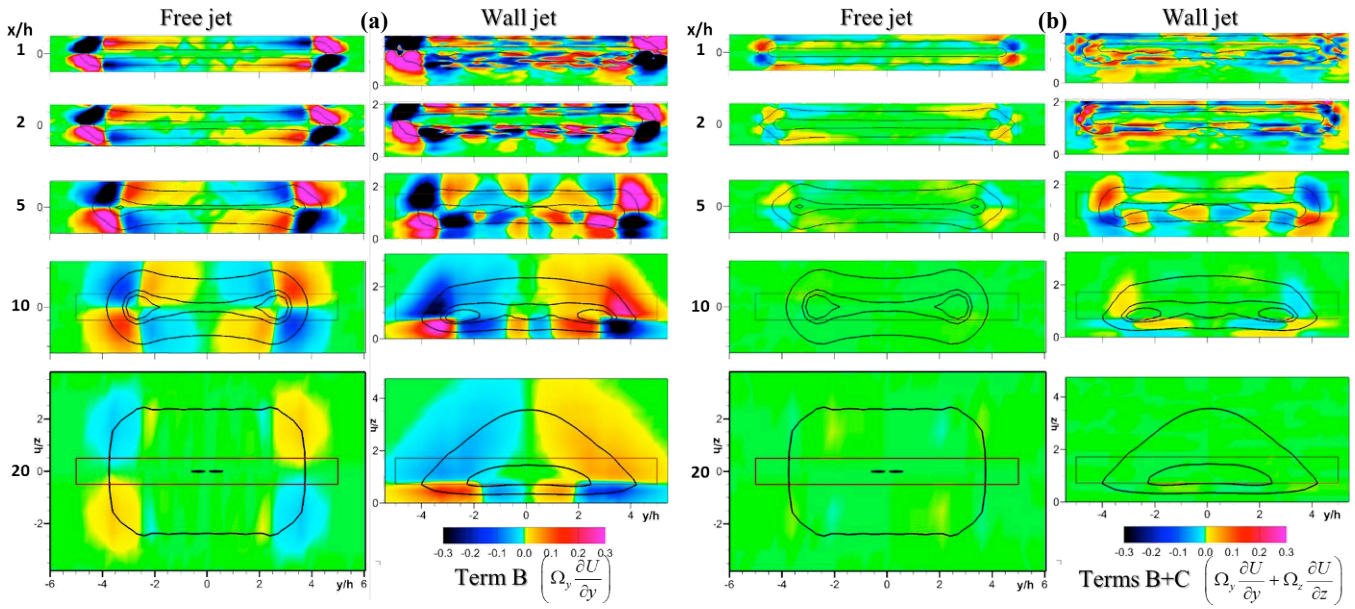

Figure 7. Contour plots of vorticity budget equation terms on cross planes at distances x/h from exit: (a) Term B, (b) Terms B+C.

previously, has corresponding effects on Ω_z and at the farthest from the exit locations, the curvature of the outer shear layer results in the development of two inclined areas with relatively high lateral vorticity of opposite signs on the sides of the lateral central axis.

VORTICITY BUDGET

Although several previous investigations have identified similar features with the present work for free and wall jets, there is still no consensus on the mechanisms leading to specific characteristics (Yu and Girimaji, 2005). To investigate the influence of the axial vorticity (Launder and Rodi, 1983) on the formation of the saddleback profiles and the dumbbell shape, consideration is given to the mean axial vorticity equation:

$$\frac{D\Omega_X}{Dt} = \underbrace{\Omega_X \frac{\partial U}{\partial x}}_{A} + \underbrace{\Omega_Y \frac{\partial U}{\partial y}}_{B} + \underbrace{\Omega_Z \frac{\partial U}{\partial z}}_{C} + \underbrace{\frac{\partial^2}{\partial y \partial z}\left(\overline{w^2} - \overline{v^2}\right) + \frac{\partial^2}{\partial y^2}\left(\overline{vw}\right) - \frac{\partial^2}{\partial z^2}\left(\overline{vw}\right)}_{D} + \underbrace{\nu\left(\frac{\partial^2 \Omega_X}{\partial y^2} + \frac{\partial^2 \Omega_X}{\partial z^2}\right)}_{E} \quad (1)$$

The three terms A, B and C on the RHS represent vorticity amplification / attenuation due to streamwise stretching / bending. The term D represents the contributions from the Reynolds stresses whereas E represents viscous dissipation.

Except for the terms B and C, the measurable terms on the RHS of eq. (1) present rather low values, whereas the terms B and C attain similar absolute values with different sign in most cases. The Term B (Fig. 7.a), in the free jet case, presents distributions which seem to be responsible for drawing fluid away from the centerline of the jet in patterns compatible with the development of the saddle back profiles and the dumbbell shape. In the wall jet case a more complicated pattern is observed which is compatible with the distorted mean axial velocity flow field in the presence of the wall. The Term C distributions (not presented) are very similar to those of the Term B with opposite signs. Therefore, the combined effect of the sum of these terms (Fig. 7.b) is in general an order of magnitude lower than the individual terms, although similar remarks may be advanced. Based on the available information it remains an open question at this stage whether the distributions of Terms B and C are the cause or the result of the mean velocity distribution and the development of the axial vorticity field in the jet.

CONCLUSIONS

Computer interpolation techniques on available 3D experimental measurements are used to further exploit previously available velocity data, which provide information on the vorticity distributions in turbulent rectangular free and wall jets. The development of the sharp-edged jets of aspect ratio 10 are characterized by mean axial velocity distributions with a predominantly "dumbbell" outline, presenting two off centre peaks, referred to as saddle back profile. Both the free and the wall jets are characterised by a contraction in the spanwise direction (parallel to the large axis of the orifice) and spreading in the lateral direction (that of the small axis of the orifice) which in the case of the free jet leads to axis switching. Unique characteristics of the wall jet are the attraction of the jet downstream, towards the wall due to a Coanda effect and a consequent distortion of the dumbbell shape. The streamwise vorticity seems to significantly affect the development of the jet. At the first stations, the emergence of a system of four corner vortices from the orifice with alternating vorticity is apparent, which is associated with the development of the dumbbell shape. The presence of the wall, results downstream in the distortion of this vortex system and the displacement of the wall side vortices towards the centre of the wall whereas, the far from the wall vortices dominate the outer layer. The transverse vorticity components are mostly dictated by the streamwise velocity

gradients across the shear layers developing around velocity peaks, and for the wall jet at the farthest downstream locations, the spanwise vorticity component close to the wall becomes dominant due to the wall shear layer. The presented terms of the longitudinal vorticity budget provide insight regarding the interaction of the jet flow structures although their contribution does not seem sufficient to fully explain the role of vorticity in flow development.

ACKNOWLEDGMENTS

AP and RRS acknowledge the Natural Sciences and Engineering Research Council of Canada and Queen's University for funding the original work and for continued support to AP. TP acknowledges the support of the University of Patras. Both AP and TP appreciate the support of the Mechanical Engineering and Aeronautics Department of the university of Patras for hosting AP during a recent sabbatical. We also acknowledge the diligent efforts of Mr. Giuseppe Garro for the many hours spent to digitize the wall jet data from the hard copy contained in Dr. Schwab's thesis.

REFERENCES

Agelin-Chaab, M., 2010, *Experimental Study of 3D Offset Jets and Wall Jets*, Ph.D. Thesis, Univ. Manitoba, Winnipeg, Canada.

Dimotakis, P., 2000, "The mixing transition in turbulent flows", *J. Fluid Mech.* Vol. 409, pp. 69-98.

Fellouah, H. and Pollard, A., 2009, "The velocity spectra and turbulence length scale distributions in the near to intermediate regions of a round free turbulent jet", *Phys. Fluids,* Vol. 21, 115101.

Launder, B. E. and Rodi, W., 1983, "The turbulent wall jet – Measurements and modelling", *Annual Review of Fluid Mechanics,* Vol. 15, pp. 429-459.

Panidis, Th., Pollard, A. and Schwab, R. R., 2016, "Vorticity component distributions in the near field of a wall jet" *Proceedings, 12th Intl. Conf. on Heat Transfer, Fluid Mechanics and Thermodynamics*, Malaga, Spain.

Schwab, R. R., 1986, *An Experimental and Numerical Investigation of 3D Jet Flows from Sharp-Edged Orifices,* Ph.D. Thesis, Queen's University, Kingston, Canada.

Vouros, A., Panidis, Th., Pollard, A. and Schwab, R. R., 2015, "Near field vorticity distributions from a sharp-edged rectangular jet", *Intl. J. Heat & Fluid Flow,* Vol. 51, pp. 383-394.

Yu, H., Girimaji, S., 2005, "Near-field turbulent simulations of rectangular jets using lattice Boltzmann method", *Phys. Fluids*, Vol. 17, 125106